DOI: 10.1002/ejic.200701351

Synthesis, Radiolabelling and Confocal Fluorescence Microscopy of Styrene-Derivatised Bis(thiosemicarbazonato)zinc and -copper Complexes

Jason P. Holland,*[a] Peter J. Barnard,[a] Simon R. Bayly,[a,b] Helen M. Betts,[a] Grant C. Churchill,[c] Jonathan R. Dilworth,*[a] Ruth Edge,[d] Jennifer C. Green,*[a] and Rebekka Hueting[a]

Keywords: Metal chelates / Radiopharmaceuticals / Density functional calculations / Hypoxia / Fluorescent probes

The synthesis of zinc(II) and copper(II) complexes of an unsymmetrical bis(thiosemicarbazonato) ligand containing a reactive styrene group are reported. The compounds have been characterised by a range of techniques including reverse-phase HPLC, cyclic voltammetry, NMR, UV/Vis, electron paramagnetic resonance and fluorescence emission spectroscopy. Time-dependent density functional theory calculations have been used to assign the electronic absorption spectrum of [Zn^{II}ATSM] and probe the nature of the fluorescent excited state. Electrochemistry experiments show that the copper(II) complex undergoes quasi-reversible one-electron reduction at biologically accessible potentials and is within the range proposed for the complex to be hypoxia-selective. The copper-64 radiolabelled complex has been prepared in aqueous solution and characterised by reverse-phase radio-HPLC. Cellular uptake in HeLa cells has been observed using confocal fluorescence microscopy.

Introduction

Since the 1950s, metal complexes of tetradentate, N_2S_2 bis(thiosemicarbazone) proligands have been the subject of intense research due to their diverse range of biological activity, including antimicrobial and antitumour properties.[1–8] More recently, radiolabelled copper(II) complexes of bis(thiosemicarbazonato) ligands have been investigated for use as hypoxia-selective radiopharmaceuticals for in vivo imaging and therapy.[7–9] In particular, the positron emitting copper-64 radiolabelled complex of 2,3-butanedione bis(4-methylthiosemicarbazonato) ligand, [Cu^{II}ATSM], has emerged as a leading hypoxia-selective compound and has received United States Food and Drug Administration (US-FDA) approval for multicentre trials imaging patients with cervical cancer.[10–12] Obata et al. have also studied [$^{64}Cu^{II}$ATSM] as a promising hypoxia-selective radiotherapeutic agent.[13]

[a] Chemistry Research Laboratory, Department of Chemistry, University of Oxford,
12 Mansfield Road, Oxford, OX1 3TA, UK
E-mail: jason.holland@chem.ox.ac.uk
jon.dilworth@chem.ox.ac.uk
jennifer.green@chem.ox.ac.uk
[b] Siemens Oxford Molecular Imaging Laboratory, Inorganic Chemistry Laboratory, University of Oxford,
South Parks Road, Oxford, OX1, UK
[c] Department of Pharmacology, University of Oxford,
Mansfield Road, Oxford, UK, OX1 3QT, UK
[d] EPSRC National Service for EPR Spectroscopy, School of Chemistry, The University of Manchester,
Oxford Road, Manchester, M13 9PL, UK

Supporting information for this article is available on the WWW under http://www.eurjic.org or from the author.

Recently, we developed a new method for the synthesis of functionalised unsymmetrical bis(thiosemicarbazonato) complexes and facile copper-64 radiolabelling by transmetallation from the corresponding zinc(II) analogues.[14] Density functional theory (DFT) calculations have also been used to probe the mechanism of hypoxia-selectivity and develop the rationale for designing new complexes with improved biodistribution characteristics.[15] Further work has investigated the origins of hypoxia-selectivity, which is thought to involve a delicate balance between one-electron reduction, protonation and ligand dissociation.[16–19] Zinc(II) bis(thiosemicarbazonato) complexes are weakly fluorescent and their in vitro uptake in various cell lines has been studied using confocal fluorescence microscopy.[14,20]

This paper describes the synthesis and characterisation of new unsymmetrical bis(thiosemicarbazonato)zinc(II) and -copper(II) complexes derivatised with a terminal styrene functional group. The styrene group has the potential to be labelled simultaneously with fluorine-18 and a biologically active molecule (BAM). The copper-64 radiolabelled complex has been prepared. Confocal fluorescence microscopy was used to study the uptake and localisation of the zinc(II) complex in the human cervical carcinoma-derived cell line, HeLa.

Results and Discussion

Unsymmetrical zinc(II) and copper(II) complexes derivatised with a terminal styrene functional group have been

synthesised (Scheme 1). Compound **3** was isolated in 66% yield as a white microcrystalline solid and was treated with 2,3-butanedione mono(4-ethylthiosemicarbazone) to give the unsymmetrical proligand **4** in 79% yield.[14,21–23] The metal complexes **5** and **6** were obtained in excellent yields from reaction of proligand **4** with a slight excess of $Zn(OAc)_2{\cdot}2H_2O$ and $Cu(OAc)_2{\cdot}H_2O$ salts, respectively. All characterisation data are consistent with the structures proposed.

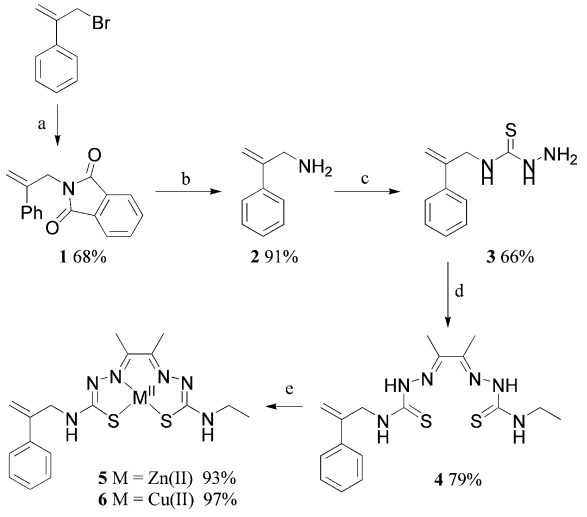

Scheme 1. Synthesis of unsymmetrical bis(thiosemicarbazonato)-zinc(II) and -copper(II) complexes **5** and **6**. (a) Potassium phthalimide, RTP, DMF, 18 h. (b) 5 equiv. hydrazine in ethanol, reflux, 1 h. (c) CS_2, NaOH(aq.) RTP, 18 h followed by 1 equiv. sodium chloroacetate, RTP, 20 h, then excess hydrazine, reflux, 4 h. (d) 1 equiv. diacetyl-2-(4-*N*-ethyl-3-thiosemicarbazone), concd. aqueous HCl, cat., stirred at 45 °C for 18 h in ethanol. (e) 1.2 equiv. of either $Zn(OAc)_2{\cdot}2H_2O$ or $Cu(OAc)_2{\cdot}H_2O$, reflux, 4 h methanol.

The isolation of 2,3-butanedione mono(4-ethylthiosemicarbazone) is the key step in the synthesis of unsymmetrical proligands.[14] Synthesis is often complicated by the formation of cyclic by-products which may be removed by recrystallisation from hot ethanol/water.[14,24,25] X-ray crystal structures of 2,3-butanedione mono(4-ethylthiosemicarbazone) and of the cyclic by-product, 4-ethyl-6-methyl-5-methylene-4,5-dihydro-1,2,4-triazine-3(2*H*)-thione have been obtained. Full crystallographic details are presented in the electronic Supporting Information (ESI).

The transmetallation of complex **5** with one equivalent of $Cu(OAc)_2{\cdot}H_2O$ in dimethyl sulfoxide (DMSO) afforded the copper(II) complex **6** and copper(II) complexation was confirmed by reverse-phase HPLC, UV/Vis and fluorescence emission spectroscopy. The change in the UV/Vis absorption and fluorescence emission spectra during titration of 3.0 mL of 0.05 mM **5** in DMSO, with one equivalent of 2.0 mM $Cu(OAc)_2{\cdot}H_2O$ in DMSO are shown in Figure 1, (a) and (b), respectively. The UV/Vis spectrum of **5** shows two peaks of similar absorbance at 437 nm (ε/M^{-1} cm^{-1} = 11328) and 319 nm (ε = 13900). The UV/Vis spectrum of **6** is typical of bis(thiosemicarbazonato)copper(II) complexes and exhibits two peaks at 478 nm (ε = 6490) and 315 nm (ε = 19414) with two low-energy shoulders at 525 nm (ε = 3698 M^{-1} cm^{-1}) and 355 nm (ε = 10571), respectively. During the transmetallation reaction, two isosbestic points are observed (Figure 1, **a**) at 471 and 384 nm which indicates that substitution of zinc(II) for copper(II) proceeds cleanly with no intermediate chromophores.[14] The UV/Vis spectrum of [Cu^{II}ATSM] has been described previously and assigned using time-dependent DFT calculations.[14,26] The zinc(II) complex **5** has a peak fluorescence emission at 524 nm with a quantum yield in DMSO of 0.018 measured relative to the emission of $[Ru(bipy)_3][PF_6]_2$, which has a quantum yield of 0.042 in water. Complex **6** is paramagnetic and consequently, transmetallation results in a linear decrease in fluorescence emission intensity as the concentration of **5** decreases (Figure 1, **b**).

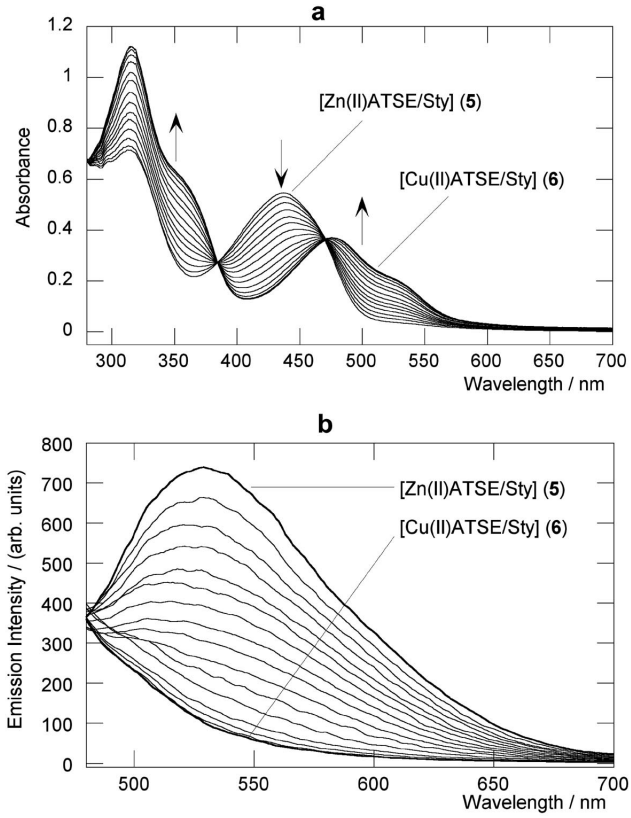

Figure 1. (a) Experimental UV/Vis absorption spectra and (b) fluorescence emission spectra (λ_{ex} = 380 nm) of 3 mL of 0.05 mM **5** (red) in DMSO on titration with sixteen, 5 μL aliquots of 2.0 mM $Cu(OAc)_2{\cdot}H_2O$ in DMSO (1.06 equiv. of copper) to give the copper(II) complex **6**. For the UV/Vis spectra, the first spectrum after the zinc(II) complex represents the addition of 15 μL (3 aliquots) of $Cu(OAc)_2{\cdot}H_2O$.

Solution phase electron paramagnetic resonance (EPR) spectra of the copper(II) complex **6** were recorded in DMF at room temperature and 100 K (Figure 2). The room temperature spectrum was simulated with EasySpin using the fast-motion regime.[27] The Kivelson formula was used to describe m_I-dependent Lorentzian line broadening [Equation (1)]. From the best fit of the simulated spectrum the optimised line-broadening parameters were found to be, a = 2.400, b = 1.347 and c = 0.512 with g_{iso} = 2.058, and a copper-63 hyperfine coupling constant of A_{iso}(Cu) = 92 G.

The room temperature spectrum exhibits superhyperfine coupling to two equivalent donor nitrogen atoms with $A_{iso}(N)$ = 16 G which results in the observed 1:2:3:2:1 coupling pattern. In the simulation it was assumed that the copper ion was copper-63. However, the copper acetate used was a mixture of copper-63 and copper-65 in natural abundance (69.17 and 30.83% respectively).[28] These two isotopes have slightly different nuclear magnetic moments of 2.22 and 2.38, respectively, which may account for minor differences observed between the experimental and simulated EPR spectra.

$$\Gamma(m_I) = a + bm_I + cm_I^2 \quad (1)$$

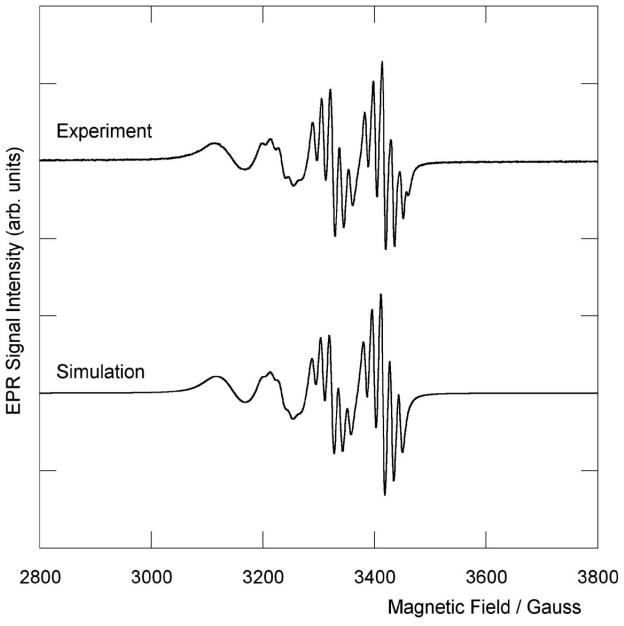

Figure 2. Room temperature experimental and simulated solution phase EPR spectra of [Cu^{II}ATSE/Sty] (**6**) in DMF recorded at 9.45623 MHz. Simulation was performed using EasySpin.[27]

The frozen solution spectrum was simulated using WinEPR Simfonia[29] to give the values, $g(x) = g(y) = 2.027$, $g(z) = 2.112$, with hyperfine coupling constants, $A_{Cu}(x) = A_{Cu}(y) = 43$ G, $A_{Cu}(z) = 194$ G, and superhyperfine coupling to the two equivalent donor nitrogen atoms of $A_N(x) = A_N(y) = 17.5$ G, $A_N(z) = 15$ G. Low g-values are indicative of the covalent nature of the bonding in copper(II) bis(thiosemicarbazonato) complexes.[26,30]

The copper-64 radiolabelled complex, ^{64}Cu-**6** was prepared in aqueous solution by transmetallation from the zinc(II) complex **5** using $^{64}Cu(OAc)_2$ (aq.). After stirring for 30 min at room temperature, a single peak was observed in the radio-HPLC chromatogram and the radiochemical yield was found to be >98%. This demonstrates that transmetallation is a facile and efficient method for radiolabelling complexes with copper radionuclides. The kinetics of the reaction have been investigated previously.[14]

The mechanism of hypoxia-selectivity of bis(thiosemicarbazonato)copper(II) complexes is thought to involve an initial one-electron reduction to give an anionic copper(I) species which may undergo oxidation by dioxygen, protonation or ligand dissociation.[16–18,31] Dearling et al. showed that hypoxia-selectivity correlated with one-electron reduction potentials for a series of fifteen aliphatic copper complexes, and suggested that complexes with reduction potentials, $E° \leq -0.58$ V, are likely to be hypoxia-selective. DFT studies support this conclusion and show that electron-donating substituents on the ligand backbone, reduce the stability of the copper(I) anion, thereby lowering the reduction potential.[16,17] The cyclic voltammogram of a 1.0 mM solution of **6** recorded at 50 mV s^{-1} scan-rate, in anhydrous, deoxygenated DMF, with 0.1 M tetrabutylammonium tetrafluoroborate electrolyte is shown in Figure 3. The complexes undergoes quasi-reversible, Cu^{II}/Cu^{I}, one-electron reduction at $E_{1/2}$(SCE) = –0.632 V. In the same experimental set-up, [Cu^{II}ATSM] has a half-wave potential of –0.646 V, which suggests that on the basis of redox potential, complex **6** may be hypoxia-selective.

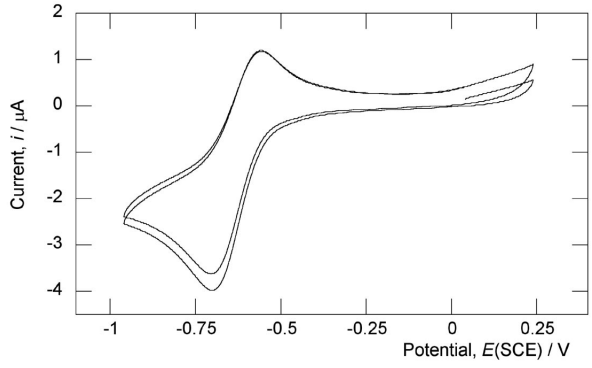

Figure 3. Cyclic voltammogram of the quasi-reversible Cu^{II}/Cu^{I} one-electron reduction of **6** in anhydrous, deoxygenated DMF recorded at 50 mV s^{-1} at room temperature. $E_{1/2}$(SCE) = –0.632 V, ΔE_p = 136 mV and $|i_{pa}|/|i_{pc}|$ = 0.72.

Time-Dependent DFT Calculations

The weak fluorescence of bis(thiosemicarbazonato)zinc(II) complexes has been used in this work and previously reported work to investigate cellular uptake and localisation in human tumour cell lines.[14,20] However, the nature of the excited state, and assignment of the electronic absorption spectrum has not been reported previously and DFT calculations have not been used to investigate the electronic structure of bis(thiosemicarbazonato)zinc(II) complexes. In order to facilitate a better understanding of the nature of the electronic transitions occurring in the zinc(II) complexes, TD-DFT calculations were conducted using ADF2006.01.[32] The experimental UV/Vis spectra of complex **5** and [Zn^{II}ATSM] are quantitatively very similar.[14] Therefore, to simplify the calculations, [Zn^{II}ATSM] was used as a model. Vertical transition energies and oscillator strengths were calculated for the first 20 singlet excited states and the simulated electronic absorption spectrum was calculated using the SWizard program.[33] The simulated

spectrum was deconvoluted as the sum of Gaussian-shaped bands using the global half-band width of $\Delta_{1/2,I}$ = 6000 cm^{-1}.[14] Figure 4 shows an overlay of the experimental UV/Vis spectrum with the deconvoluted simulated TD-DFT spectrum. Several different exchange-correlation functionals were used. However, only minor differences were observed and the best fit with the experimental data of both calculated relative absorbance and calculated peak energies was found using BP86 with the TZ2P basis set. Further details are given in the ESI.

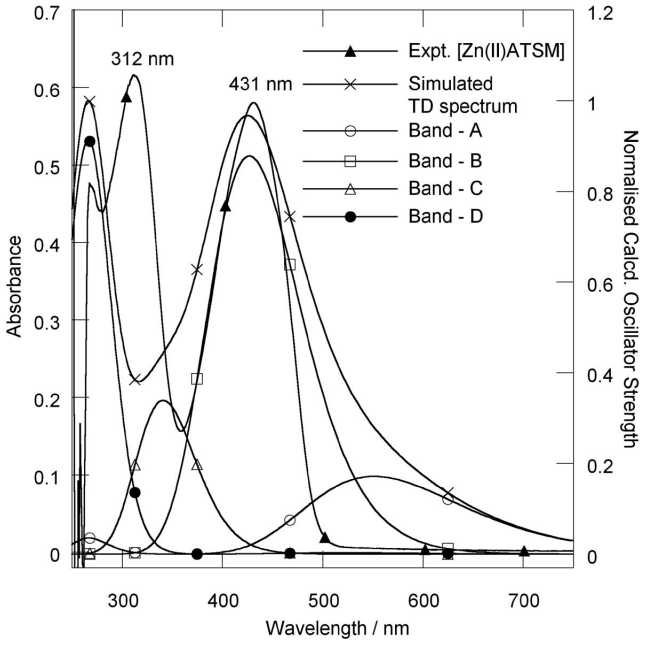

Figure 4. Experimental and TD-DFT-simulated electronic absorption spectra for [Zn^{II}ATSM]. BP86/TZ2P methodology was used in the DFT calculation.

The experimental UV/Vis spectrum recorded in DMF shows two peaks at 431 (ε/$M^{-1}cm^{-1}$ 11266) and 312 (ε = 11978). The calculated gas-phase TD-DFT spectrum (Figure 4) is in good agreement with the experimental spectrum, particularly in the visible region. Two peaks of similar intensity are predicted at 427 nm and 265 nm. The simulated spectrum has been deconvoluted as four major absorption bands. These bands have been assigned to transitions from the ground electronic state to calculated excited states (Table 1). Each of the excited states is then expressed in terms of rearrangement in the electron density of the ground state molecular orbitals, from which the nature of the electronic transition may be deduced and the spectrum assigned. The simulated peak at 265 nm is blue-shifted by 47 nm in comparison to the absorption band observed experimentally. However, considering that calculated absorption band at 265 nm is composed of transitions to more than 6 excited states with non-zero oscillator strengths (Table 1), the calculations provide a good model for the experimental spectrum.

Figure 5 shows a molecular orbital diagram, along with the main orbitals involved in the transitions associated with the calculated absorption bands A–D (Figure 4 and Table 1). Molecular-orbital assignment reveals that in contrast to the copper(II) complex,[14,15] [Cu^{II}ATSM], the frontier orbitals and the calculated bands involve mainly ligand-based ππ* orbitals. On electronic excitation, there is in general a redistribution of electron density of the π system from the sulfur atoms towards the carbon–carbon backbone. In particular, transitions to excited states 1 and 4, corresponding to the lowest energy bands A and B in the visible region, involves redistribution of electron density from the sulfur lone-pairs to the C–C ππ* orbitals. The HOMO–LUMO energy gap, Δ, is 1.87 eV and corresponds to the major molecular orbital transition in band A. The calculated oscillator strength of the transition to excited state 1, is larger than that observed in the experimental UV/Vis spectrum.

Fluorescence emission observed for the bis(thiosemicarbazonato) zinc(II) complexes is likely to occur from excited state 1. TD-DFT calculations suggest that radiative emission occurs from an excited state with large ligand-based ππ* (LUMO) character to the ground state and involves relaxation of excited lone-pairs of electrons on the sulfur atoms. The peak fluorescence emission for most bis(thiosemicarbazonato)zinc(II) complexes occurs around 535 nm.[14,20] This energy is consistent with the calculated energy for band A of 552 nm. For in vivo imaging, it is

Table 1. Excited state and molecular orbital deconvolution of the TD-DFT simulated electronic absorption spectrum of [Zn^{II}ATSM].

Absorption band[a]	Excited states	Oscillator strength	λ_{ex} (calcd.)	Molecular orbital contributions (%) HOMO [*m*]	LUMO [*n*]	Percentage contribution (%)	Assignment[b]
		f	[nm][b]				
A	1	0.048	552	0	0	81	ligand-based ππ*
				–2	0	18	sulfur *p*π to ππ*
B	4	0.245	427	–2	0	79	sulfur *p*π to ππ*
				0	0	15	ligand-based ππ*
C	6 and 7	0.095[c]	341[d]	–6	0	78[e]	Zn^{II} ligand σ* to ligand ππ*
				–5	0	22	ligand-based ππ*
D	10, 11, 14, 15, 18 and 19	0.308[c]	265[d]	0	+1	60[e]	ligand-based ππ*
				0	+2	10	ligand-based ππ*
				0	+5	12	ligand-based ππ*

[a] Figure 4. [b] For the MO assignment, only orbital contributions >10% have been included. [c] Sum of individual oscillator strengths. [d] Weighted average using oscillator strengths. [e] Percentage contributions corrected for individual oscillator strengths.

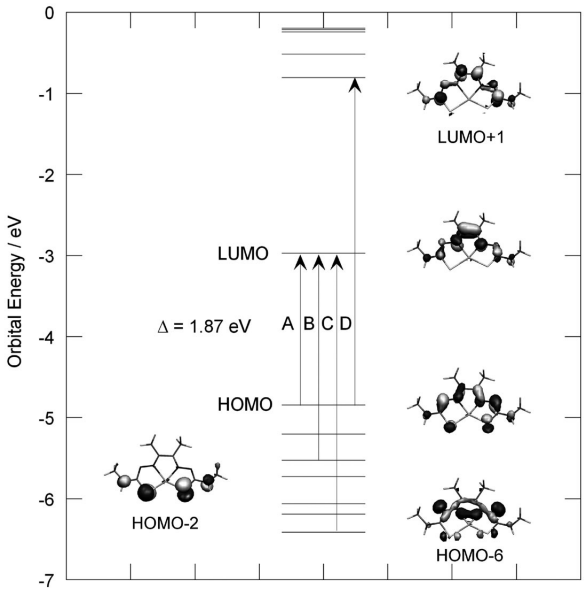

Figure 5. Molecular orbital diagram showing transitions from the occupied to virtual orbitals along with molecular orbital isosurfaces of the LUMO+1, LUMO, HOMO, HOMO-2 and HOMO-6. The arrows labelled A–D represent the major molecular orbital transition associated with each of the four calculated absorption bands (Table 1). Fluoresence emission corresponds mainly to the LUMO→HOMO relaxation and the emission peak at 535 nm is coincident with the energy of calculated absorption band A (Figure 4 and Table 1).

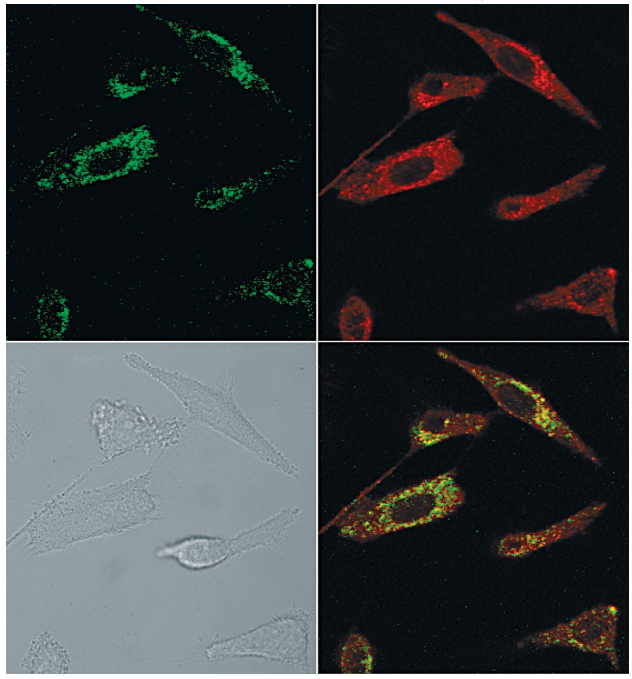

Figure 6. Confocal fluorescence microscopy images of HeLa human cervical carcinoma cells in DMEM medium; (top left) fluorescence image of the zinc(II) complex **5** (λ_{ex} = 488 nm, λ_{em} = 530 nm); (top right) fluorescence image of LysoTracker Red™ (λ_{ex} = 568 nm, λ_{em} = 605 nm); (bottom left) brightfield image; (bottom right) co-localisation of complex **5** and LysoTracker Red™ fluorescence. Nuclei are visible as the spherical regions within the cells showing no fluorescence emission.

desirable to tune the emission wavelength and develop fluorophores which emit at wavelengths >600 nm. Calculations presented here suggest that ligands with π-accepting groups on the backbone would result in a red-shift in the peak emission wavelength. Work is underway designing new fluorescent probes based on both bis(thiosemicarbazonato)copper(II) and -zinc(II) complexes for in vitro imaging.

Confocal Microscopy

For a new compound to be considered as a potential radiopharmaceutical for in vivo imaging and therapy, it is important to understand cellular uptake and biodistribution properties. Confocal and epifluorescence microscopy have been used to study structure–activity relationships for a range of bis(thiosemicarbazonato)zinc(II) complexes.[14,20] Cellular uptake and intracellular localisation of complex **5** in HeLa human cervical carcinoma cells was studied using confocal fluorescence microscopy under normal atmospheric oxygen concentrations. Cells were incubated with 100 μM of **5** at 37 °C for 30 min prior to image acquisition (Figure 6). The mechanism of intracellular trapping is thought to involve protonation.[15,19] Therefore, after recording the fluorescence of **5** the sample was incubated with LysoTracker™, a fluorophore which localises in acidic organelles, such as lysosomes and endocytotic vesicles.

The images demonstrate that during the course of the in vitro experiments, complex **5** remains intact and is taken up by HeLa cells. In control experiments, the proligand, H_2ATSE/Sty, and zinc(II) dichloride were found to be non-fluorescent.[20] Complex **5** is mainly distributed within the cytosol, showing no nuclear uptake. Co-localisation experiments with LysoTracker™ reveal significant overlap between acidic compartments and the intracellular distribution of **5** which provides evidence to support the involvement of a protonation step in the mechanism of uptake and trapping. Further investigations are underway looking at the role of diffusion and receptor-mediated endocytosis in mechanism of cellular uptake.

Dual Labelling and Functionalisation

In previous work, a methodology for functionalising bis(thiosemicarbazonato) complexes with biologically active molecules was presented.[14] PET imaging studies suggest that in vivo biodistribution, localisation and excretion pathways can be modified by controlling the nature of the BAM substituents. In addition, PET experiments indicate that for several bis(thiosemicarbazonato) copper(II) complexes, the ligand may dissociate, releasing the copper radionuclide into the normal pathways of copper metabolism. It is important to understand where and under what conditions ligand dissociation may occur. The new

styrene functional group offers the potential of studying ligand dissociation in vivo by a combination of dual labelling and functionalisation with a BAM (Scheme 2).

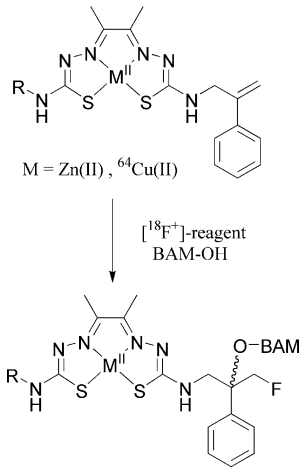

Scheme 2. Proposed reaction scheme for radiolabelling with either copper-64 or fluorine-18 radionuclides and functionalisation of [Cu^{II}ATSR/Sty] with a biologically active molecule (BAM). [^{18}F^{+}] represents fluorine-18 radiolabelled electrophilic fluorinating reagents.[36]

The bis(thiosemicarbazonato)zinc(II) complexes with a pendent styrene moiety could be radiolabelled with either copper-64 or fluorine-18.[34,35] Electrophilic fluorination-nucleophilic addition reactions are well known and the reactions of NF-fluorinating reagents with a wide range of functional groups such as carbanions, aromatic compounds, α-fluorination of sulfides, glycals and alkenes, including styrene, have been investigated.[36,37] In particular, NF-fluorinating reagents such as *N*-fluorobenzenesulfinimide (NFSi) and 1-chloromethyl-4-fluoro-1,4-diazoniabicyclo[2.2.2]-octane (Selectfluor^{TM}) react with styrene derivatives with Markovnikov-type regioselectivity in high yields.[36,38] More recently, Gouverneur and co-workers have prepared fluorine-18 radiolabelled reagents such as [^{18}F]-*N*-fluoro-benzenesulfinimide ([^{18}F]-NFSi), and used these to prepare potential radiopharmaceuticals.[39] Initial experiments are encouraging and investigations looking at the preparation of functionalised bis(thiosemicarbazonato) complexes radiolabelled with copper-64 or fluorine-18 are underway.

Conclusions

Zinc(II) and copper(II) complexes of a new unsymmetrical bis(thiosemicarbazonato) ligand providing a reactive styrene functional group have been synthesised. The copper-64 radiolabelled complex has been prepared in aqueous solution by transmetallation from the corresponding zinc(II) complex. Confocal fluorescence microscopy has also been used to investigate the cellular uptake and intracellular distribution of the zinc(II) complex. In addition, TD-DFT calculations have been used to assign the electronic absorption spectrum of bis(thiosemicarbazonato)-zinc(II) complexes. The simulated spectrum is in excellent agreement with the experimental UV/Vis spectrum of [Zn^{II}ATSM] and the calculations provide information about the nature of the fluorescent excited state.

A potential synthetic route for simultaneous fluorination, functionalisation with biologically active molecules and dual radiolabelling with either copper-64 or fluorine-18, of the styrene-derivatised bis(thiosemicarbazonato) complex is presented. Experiments investigating electrophilic fluorination-nucleophilic addition to the styrene moiety are underway.

Experimental Section

General: All reagents and solvents were obtained from commercial sources (Sigma–Aldrich and Lancaster) and unless otherwise stated, were used as received. Elemental analyses were performed by the microanalysis service of the department at the University of Oxford. NMR spectra were recorded with a Varian Mercury VX300 spectrometer, [^{1}H at 300 MHz, ^{13}C(^{1}H) at 75.5 MHz] using the residual solvent signal as an internal reference. Mass spectra were recorded with a Micromass LCT Time of Flight Mass Spectrometer using positive ion electrospray (ES^{+}). Where possible, accurate masses are reported to four decimal places using tetraoctylammonium bromide (466.5352 Da) as an internal reference. UV/Vis spectra were recorded with a Perkin–Elmer Lambda 19 UV/Vis/near-IR spectrometer. Fluorescence emission spectra were recorded with a Hitachi F-4500 Fluorescence spectrophotometer. EPR spectra were recorded using quartz flat cells (1 or 2 mm cavity) with a Bruker EMX-micro X-band spectrometer at the EPSRC National EPR Service, at the University of Manchester. High performance liquid chromatography (HPLC) was conducted using a Gilson HPLC machine equipped with a Hamilton PRP-1 reverse phase column and UV/Vis detection at 254 nm. Retention times, R_t [min], using a water/acetonitrile gradient elution method (1.0 mL/min), shown in the Supporting Information, are presented for all compounds. Where stated in the experimental section, trifluoroacetic acid (TFA) was use as an ion pair agent. Cyclic voltammograms of approximately 1.0 mM solutions of zinc(II) and copper(II) complexes in 5.0 mL anhydrous dimethylformamide (DMF) were recorded with a CH Instruments Electrochemical Analyser using a platinum working electrode, a platinum wire counter/auxiliary electrode and a silver/silver ion reference electrode. Ferrocene was used as an internal reference for which the one-electron redox process occurs at $E_{1/2}$ = 0.53 V (DMF) vs. SCE.

Zinc(II) Complex of 2,3-Butanedione Bis(4-methylthiosemicarbazone), [Zn^{II}ATSM]: This compound was synthesized in accordance with a previously reported procedure.[40] ^{1}H NMR (300 MHz, [D$_6$]DMSO): δ = 7.21 (br. s, 2 H, CH$_3$N*H*), 2.83 and 2.81 (6 H, two overlapping singlets, C*H*$_3$NH), 2.20 (s, 6 H, C*H*$_3$C=N) ppm. MS (ES^{+}): *m*/*z* (calcd.) 323.0104 (323.0091) = {M + H^{+}}. λ_{max} (DMF) = 431 (ε / M^{-1}cm^{-1} 11266), 312 nm (11978). HPLC: R_t = 10.40 min (flow rate: 0.9 mL/min).

***N*-(2-Phenylallyl)phthalimide (1):** The synthesis was based on a procedure described by Sheehan and Bolhofer.[21] Potassium phthalimide (2.42 g, 0.0131 mol) was added to a solution of 3-bromo-2-phenylpropene (cinnamyl bromide) (2.34 g, 0.0118 mol) in 20 mL DMF at room temperature. The reaction was slightly exothermic and the temperature increased from 21.5 °C to 46.5 °C during the first 5 min. Then it was cooled slowly to room temperature and stirring was continued for 18 h, after which time the mixture turned a dark brown/orange colour and a white precipitate formed. Chlo-

roform (30 mL) (or dichloromethane, DCM) was added and the mixture was poured onto 100 mL of deionised water. The aqueous phase was separated and extracted three times with 30 mL portions of chloroform (or DCM). The combined organic extract was then washed with 20 mL NaOH (aq.) (0.2 M) and dried with anhydrous magnesium sulfate. The chloroform (or DCM) was removed in vacuo at 40 °C and the crystalline residue was triturated with 30 mL of cold diethyl ether. The colourless, crystalline product was isolated by filtration (2.11 g, 8.01 mmol, 68%); m.p. 118–119 °C (ref.[22] 116–117 °C). $C_{17}H_{13}NO_2$ (263.09): calcd. C 77.5, H 5.05, N 5.3; found C 77.55, H 5.0, N 5.3. ^{1}H NMR (300 MHz, $CDCl_3$): δ = 7.78 (dd, *m*-C*H*-phthalimide, $^4J_{HH}$ = 3.1, $^3J_{HH}$ = 5.4 Hz, 2 H, A part of an AA′XX′ spin system), 7.64 (dd, *o*-C*H*-phthalimide, $^4J_{HH}$ = 3.1, $^3J_{HH}$ = 5.4 Hz, 2 H, X part of an AA′XX′ spin system), 7.30–7.10 (m, 5 H, *Ph*-), 6.58 [d, $^2J_{HH}$ = 15.9 Hz, 1 H, *trans*-CH_2=C(Ph)CH_2], 6.18 [dt, $^2J_{HH}$ = 15.9, $^3J_{HH}$ = 6.5 Hz, 1 H, *cis*-CH_2=C(Ph)CH_2], 4.37 [br. d, $^3J_{HH}$ = 6.5 Hz, 2 H, CH$_2$=C(Ph)CH_2] ppm. ^{13}C{^{1}H} NMR (75.5 MHz, [D$_6$]DMSO): δ = 167.89 (2 *C*=O), 136.16 [CH$_2$=*C*(Ph)CH$_2$], 133.92 (C5 and C6, *m*-phthalimide), 133.71 (C3 and C8, *i*-phthalimide), 132.10 (*i*-*Ph*), 128.46 (*m*-*Ph*), 127.83 (*p*-*Ph*), 126.46 (*o*-*Ph*), 123.25 (C4 and C7, *o*-phthalimide), 122.67 (*C*H$_2$=), 39.62 (*C*H$_2$N) ppm. MS (ES$^+$): *m*/*z* = 286 [M + Na$^+$]. HPLC: R_t = 17.14 min.

2-Phenylprop-2-enylamine (2): The synthesis was based on a procedure described by Abbenante and Prager.[22] Hydrazine hydrate (0.6 mL, 19.3 mmol) was added to a suspension of *N*-(2-phenylallyl)phthalimide (**1**) (1.00 g, 3.80 mmol) in ethanol (20 mL). The reaction mixture was heated under reflux for 1 h and a white precipitate formed. Then 4.0 mL of HCl(aq.) (2.0 M) was added and the reaction mixture heated under reflux for a further 1 h. Upon addition of the HCl(aq.) the white precipitate dissolved to give a colourless solution, which, after 1 min became cloudy as a white suspension of phthalyl hydrazide formed. The reaction mixture was cooled to 4 °C and the phthalyl hydrazide was removed by filtration and washed with cold ethanol (2 × 5 mL). The ethanol was removed in vacuo and the solid residue was redissolved in 15 mL NaOH(aq.) (2.0 M). The solution was extracted with diethyl ether (5 × 20 mL) and the organic extract was dried with magnesium sulfate, filtered and the solvent removed in vacuo to give the product as a colourless oil (0.46 g, 3.47 mmol, 91%). ^{1}H NMR (300 MHz, $CDCl_3$): δ = 7.30–7.10 (m, 5 H, *Ph*-), 6.45 [br. d, $^2J_{HH}$ = 15.9 Hz, 1 H, *trans*-CH_2=C(Ph)CH$_2$], 6.27 [dt, $^2J_{HH}$ = 15.9, $^3J_{HH}$ = 5.8 Hz, 1 H, *cis*-CH_2=C(Ph)CH$_2$], 3.42 [m, $^3J_{HH}$ = 5.7 Hz, 2 H, CH$_2$=C(Ph)CH_2], 1.45 (s, 2 H, NH_2) ppm. MS (ES$^+$): *m*/*z* 117 = [L + H$^+$, – NH$_3$], corresponding to the [C$_9$H$_9$]$^+$ fragment ion. HPLC: R_t = 6.76 min (TFA).

4-(2-Phenylprop-2-enyl)thiosemicarbazide (3): The synthesis was based on a procedure described by Scovill.[23] Carbon disulfide (0.19 mL, 0.24 g, 3.15 mmol) and 10 mL of a 1.05 M solution of sodium hydroxide (0.13 g, 3.25 mmol) in deionised water was added to (2-phenylprop-2-enyl)amine (**2**) (0.41 g, 3.08 mmol) in a 50 cm^3 round-bottomed flask. The reaction mixture was stirred at room temperature for 18 h. One equivalent of sodium chloroacetate (0.36 g, 3.09 mmol) was then added and stirring continued for a further 20 h at room temperature. The reaction mixture became a clear yellow colour. Excess hydrazine hydrate (0.80 mL, 0.82 g, 25.7 mmol) was added and the mixture was heated under reflux for 4 h. The colourless solution was cooled and left to stand overnight at 4 °C. A white precipitate and a brown oil formed. The product was extracted from the aqueous reaction mixture with ethyl acetate (3 × 20 mL). The organic extract was dried with magnesium sulfate and the solvent removed under reduced pressure and the product dried in vacuo to give compound **3** as a white solid (0.42 g, 2.0 mmol, 66%). ^{1}H NMR (300 MHz, $CDCl_3$): δ = 8.14 [br. s, 1 H, C(=S)N*H*NH$_2$], 7.54 [br. m, 1 H, CH$_2$N*H*C(=S)], 7.35–7.13 (m, 5 H, *Ph*-), 6.51 [br.d, $^2J_{HH}$ = 15.9 Hz, 1 H, *trans*-CH_2=C(Ph)CH$_2$], 6.22 [dt, $^2J_{HH}$ = 15.9, $^3J_{HH}$ = 6.2 Hz, 1 H, *cis*-CH_2=C(Ph)CH$_2$], 4.38 [m, $^3J_{HH}$ = 6.1 Hz, 2 H, CH$_2$=C(Ph)CH_2], 3.82 (br. s, 2 H, NH_2) ppm. ^{13}C{^{1}H} NMR (75.5 MHz, [D$_6$]DMSO): δ = 181.56 (*C*=S), 136.32 [CH$_2$=*C*(Ph)CH$_2$], 132.11 (*i*-*Ph*), 128.47 (*m*-*Ph*), 127.63 (*p*-*Ph*), 126.28 (*o*-*Ph*), 124.99 (*C*H$_2$=), 45.86 (*C*H$_2$N) ppm. MS (ES$^+$): *m*/*z* 208 = [M + H$^+$]. HPLC: R_t = 10.52 min.

2,3-Butanedione Mono(4-ethylthiosemicarbazone): This compound was prepared using a previously reported procedure.[14] 2,3-Butanedione (1.8 mL, 1.77 g, 20.5 mmol) was added to 4-ethylthiosemicarbazide (2.00 g, 16.8 mmol). The compound was isolated as a white microcrystalline solid (2.63 g, 14.0 mmol, 84%); m.p. 127–129 °C. $C_7H_{11}N_3OS$ (185.06): calcd. C 44.6, H 7.2, N 22.7, S 17.2; found C 44.9, H 7.0, N 22.4, S 17.1. ^{1}H NMR (300 MHz, [D$_6$]DMSO): δ = 10.57 [s, 1 H, C(=S)N*H*N=], 8.66 (br.t, 1 H, CH$_2$N*H*), 3.63 (m, $^3J_{HH}$ = 7.1 Hz, 2 H, CH$_3$CH_2NH), 2.42 (s, 3 H, CH_3C=O), 1.96 (s, 3 H, CH_3C=N), 1.15 (t, $^3J_{HH}$ = 7.1 Hz, 3 H, CH_3CH$_2$) ppm. ^{13}C{^{1}H} NMR (75.5 MHz, [D$_6$]DMSO): δ = 197.43 (*C*=O), 177.89 (*C*=S), 145.48 (*C*=N), 38.71 (CH$_3$CH_2), 24.72 (*C*H$_3$C=O), 14.06 (CH_3CH$_2$), 9.99 (*C*H$_3$C=N) ppm. MS (ES$^+$): *m*/*z* (calcd.) 188.0855 (188.0858) = [M + H$^+$]. HPLC: R_t = 9.67 min. Crystals suitable for single-crystal X-ray diffraction were obtained by recrystallisation from hot aqueous ethanol. A crystal of the cyclic by-product, 4-ethyl-6-methyl-5-methylene-4,5-dihydro-1,2,4-triazine-3(2*H*)-thione, suitable for single-crystal X-ray diffraction was isolated from the reaction mixture.

2,3-Butanedione 4-Ethyl-4′-(2-phenylprop-2-enyl)bis(thiosemicarbazone) (H_2ATSE/Sty, 4): 2,3-Butanedione mono(4-ethylthiosemicarbazone) (0.28 g, 1.5 mmol) was added to a stirred suspension of 4-(2-phenylprop-2-enyl)thiosemicarbazide (**3**) (0.30 g, 1.4 mmol) in 10 mL ethanol over 30 min. Then 5 drops of 10% aqueous HCl acid catalyst was added and the reaction mixture was stirred overnight at 45 °C. A white precipitate formed immediately on addition of the acid. The mixture was cooled to 4 °C for 12 h and the solid was collected by filtration, washed with ethanol (2 × 20 mL) and diethyl ether (3 × 20 mL) then dried in vacuo. Compound **5** was isolated as a cream/white powder (0.43 g, 1.1 mmol, 79%). $C_{17}H_{24}N_6S_2$ (376.15): calcd. C 54.0, H 6.4, N 21.9, S 17.5; found C 54.2, H 6.4, N 22.3, S 17.0. ^{1}H NMR (300 MHz, $CDCl_3$): δ = 10.34 [s, 1 H, NHC(=S)N*H*N=], 10.17 [s, 1 H, NHC(=S)N*H*N=], 8.66 [m, 1 H, CH$_2$=C(Ph)CH$_2$N*H*], 8.43 (m, 1 H, CH$_3$CH$_2$N*H*), 7.41 (d, $^3J_{HH}$ = 7.4 Hz, 2 H, *o*-*Ph*), 7.32 (t, $^3J_{HH}$ = 7.3 Hz, 2 H, *m*-*Ph*), 7.21 (m, $^3J_{HH}$ = 7.3 Hz, 1 H, *p*-*Ph*), 6.52 [br.d, $^2J_{HH}$ = 16.0 Hz, 1 H, *trans*-CH_2=C(Ph)CH$_2$], 6.35 [dt, $^2J_{HH}$ = 16.0, $^3J_{HH}$ = 5.4 Hz, 1 H, *cis*-CH_2=C(Ph)CH$_2$], 4.41 [m, 2 H, CH$_2$C(Ph)CH_2NH], 3.60 (m, $^3J_{HH}$ = 6.6 Hz, 2 H, CH$_3$CH_2NH), 2.23 (6 H, two overlapping singlets, CH_3C=N), 1.14 (t, 3 H, $^3J_{HH}$ = 6.9 Hz, CH_3CH$_2$NH) ppm. ^{13}C{^{1}H} NMR (75.5 MHz, [D$_6$]DMSO): δ = 177.82 (*C*=S), 177.31 (*C*=S), 148.27 (*C*=N), 147.85 (*C*=N), 136.45 [CH$_2$=*C*(Ph)-CH$_2$NH], 130.40 (*i*-*Ph*), 128.57 (*m*-*Ph*), 127.37 (*p*-*Ph*), 126.40 (*C*H$_2$=), 126.01 (*o*-*Ph*), 45.54 [CH$_2$=C(Ph)*C*H$_2$N], 38.50 (CH$_3$*C*H$_2$NH), 14.32 (*C*H$_3$CH$_2$NH), 11.74 (*C*H$_3$C=N), 11.69 (*C*H$_3$C=N) ppm. MS (ES$^+$): *m*/*z* (calcd.) 399 = [M + Na$^+$]. HPLC: R_t = 15.72 min.

Zinc(II) Complex of 4 (Zn^{II}ATSE/Sty, 5): Zinc(II) diacetate dihydrate, Zn(OAc)$_2$·2H$_2$O (0.11 g, 0.5 mmol, 1.25 equiv.) was added to compound **4** (0.15 g, 0.4 mmol) in 10 mL of methanol. Upon addition of Zn(OAc)$_2$·2H$_2$O the reaction mixture became clear orange. The mixture was then heated under reflux for 4 h and cooled overnight at 4 °C. The product was precipitated by slow ad-

dition of 20 mL deionised water, isolated by filtration, washed with water (2 × 10 mL) and dried in vacuo at 60 °C to give complex **5** as a yellow powder (0.16 g, 0.37 mmol, 93%). $C_{17}H_{22}N_6S_2Zn$ (438.06): calcd. C 46.2, H 4.9, N 18.9, S 15.1, Zn 15.3; found C 46.4, H 5.0, N 19.1, S 14.6, Zn 14.9. ^{1}H NMR (300 MHz, [D$_6$]-DMSO): δ = 7.50 [br. s, 1 H, CH_2=C(Ph)CH_2N*H*], 7.38 (d, $^3J_{HH}$ = 7.1 Hz, 2 H, *o-Ph*), 7.31 (t, $^3J_{HH}$ = 7.2 Hz, 2 H, *m-Ph*), 7.25–7.18 (m, 2 H, *p-Ph* and CH_3CH_2NH, assigned by 2D-COSY), 6.51 [d, $^2J_{HH}$ = 15.9 Hz, 1 H, *trans*-C*H*$_2$=C(Ph)CH$_2$], 6.33 [dt, $^2J_{HH}$ = 15.9, $^3J_{HH}$ = 5.8 Hz, 1 H, *cis*-C*H*$_2$=C(Ph)CH$_2$], 4.13 [m, 2 H, $CH_2C(Ph)CH_2NH$], 3.37 (2 H, assigned by 2D-COSY, CH_3CH_2NH), 2.20 and 2.18 (6 H, two overlapping singlets, C*H*$_3$C=N), 1.10 (t, $^3J_{HH}$ = 7.1 Hz, 3 H, C*H*$_3$CH$_2$NH) ppm. ^{13}C{^{1}H} NMR (75.5 MHz, [D$_6$]DMSO): δ = 175.49 (*C*=S), 144.75 (*C*=N) (only two weak quaternary resonances were observed), 136.72 [CH$_2$=*C*(Ph)CH$_2$NH], 130.10 (*i-Ph*), 128.56 (*m-Ph*), 127.47 (*p-Ph*), 127.22 (*C*H$_2$=), 126.00 (*o-Ph*), 44.08 [CH$_2$=C(Ph)*C*H$_2$N], 36.88 (CH$_3$*C*H$_2$NH), 14.60 (*C*H$_3$CH$_2$NH), 13.92 (*C*H$_3$C=N), 13.78 (*C*H$_3$C=N) ppm. MS (ES$^+$): *m*/*z* (calcd.) 439.0707 (439.0717) = [M + H$^+$]. λ_{max}(DMSO) = 437 (ε / M^{-1} cm^{-1} 11328) and 319 (13900) nm. HPLC: R_t = 15.91 min.

Copper(II) Complex of 4 (Cu^{II}ATSE/Sty, 6): Copper(II) diacetate monohydrate, Cu(OAc)$_2$·H$_2$O (63 mg, 0.32 mmol, 1.20 equiv.) was added to compound **4** (0.10 g, 0.27 mmol) in 10 mL of methanol. Upon addition of Cu(OAc)$_2$·H$_2$O the reaction mixture became dark red/brown. The mixture was then heated at 50 °C for 4 h and cooled overnight at 4 °C. The precipitate was isolated by filtration, washed with water (2 × 10 mL) and dried in vacuo at 60 °C to give complex **6** as a red/brown powder (0.11 g, 0.26 mmol, 97%). $C_{17}H_{22}CuN_6S_2$ (438.07): calcd. C 46.4, H 5.0, N 19.3, S 15.2, Cu 14.3; found C 46.6, H 5.0, N 19.2, S 14.6, Cu 14.5. MS (ES$^+$): *m*/*z* (calcd.) 438.0737 (438.0722) = [M + H$^+$]. λ_{max}(DMSO) = 525sh (ε / M^{-1} cm^{-1} 3698), 478 (6490), 355sh (10571) and 315 (19414) nm. HPLC: R_t = 20.54 min.

Copper-64 Radiolabelling: Radiolabelling experiments were conducted at the Siemens Oxford Molecular Imaging Laboratory (SOMIL). Copper-64 was provided by the Wolfson Brain Imaging Centre, Cambridge, UK, as ^{64}CuCl$_2$(aq.) in 0.1 mol dm^{-3} HCl. An aqueous solution of copper-64 acetate, ^{64}Cu(CH$_3$CO$_2$)$_2$, was prepared by diluting 0.2 mL of the ^{64}CuCl$_2$(aq.) in 0.1 M HCl with 0.1 M sodium acetate (1.8 mL, pH 5.5). This stock solution was used for the radiolabelling experiments and the activity was measured as 66.4 MBq in 2 mL.

A standard solution of **5** [Zn^{II}ATSE/Sty] was prepared by dissolving 0.5 mg in 1.0 mL of DMSO. Copper-64 radiolabelled complex ^{64}Cu-**6** was prepared by reacting ^{64}Cu(CH$_3$CO$_2$)$_2$ (200 μL, <10 MBq), with 100 μL of the standard solution of **5**, and water (400 μL) in a 2 mL reaction vial.

Reaction mixtures were stirred at room temperature for between 15 and 30 min then 25 μL of the reaction solution were taken for analysis by reverse-phase radio-HPLC. The syringe was washed thoroughly with DMSO and water both before and after use to prevent contamination. All washings were stored behind the lead shield. HPLC analysis was performed using a Gilson HPLC machine equipped with a 250 mm × 4.6 mm Phenomenox Primesphere 5 C18-HC 110H column. Both UV detection ($\lambda_{obsd.}$ = 254 nm) and NaI scintillation crystal detection were used in series with a delay time of approximately 10 s. A 25 min water/acetonitrile gradient elution method was used.

Confocal Fluorescence Microscopy: In vitro cellular uptake studies were carried out on the adherent human cervical carcinoma-derived cell line HeLa. Cells were seeded as monolayers in T75 tissue culture flasks (Nunc, Denmark) and cultured in Dulbecco's Modified Eagle's Medium (DMEM) (Sigma, UK) supplemented with 10% foetal bovine serum (HyClone, USA), L-glutamine (2 mM), 100 units/mL penicillin and 100 μg/mL streptomycin (GIBCO, Invitrogen, UK). Cells were maintained at 37 °C in a 5% CO_2 humidified atmosphere and grown to approximately 95% confluence before being split using 2.5% Trypsin (GIBCO).

Cells were seeded onto chambered coverglass (Nunc) for confocal microscopy and incubated for 12 h to ensure adhesion. **5** was dissolved in DMSO at a stock concentration of 10 mM, and diluted to a final concentration of 100 μM in phenol-free DMEM, then incubated at 37 °C for 30 min. Prior to imaging, the solution was replaced with 1 mL fresh medium. Lysotracker Red™ (Molecular Probes) co-localisation was carried out by incubating with 100 nM in DMEM for the last 5–10 min of the 30 min incubation period. Images were recorded using a Zeiss LSM 510 Meta confocal microscope, equipped with a 40x oil immersion objective (NA 1.3). The excitation/emission wavelengths for acquisition were 488/505–530 nm (Ar ion laser) for **5** and 543/560 nm (HeNe laser) for Lysotracker Red™. Fluorescence of **5** was confirmed by comparison to images of cellular auto-fluorescence in 1 mL of DMEM medium containing 0.01% DMSO.

Density Functional Theory Calculations: All calculations were conducted using density functional theory (DFT) as implemented in the ADF2006.01 suite of ab initio quantum chemistry programs.[32,41,42] Restricted geometry optimisations and vibrational frequency calculations were performed using the generalised gradient approximation with the local density approximation of Vosko, Wilk and Nusair[43] and with nonlocal exchange corrections by Becke[44] and nonlocal correlation corrections by Perdew.[45] The all electron triple-ξ TZ2P basis set was employed for all atoms. Normal SCF and geometry convergence criteria were used and no symmetry constraints were imposed. For all gas phase calculations, harmonic frequency analysis based on analytical second derivatives was used to characterize the optimised geometries as local minima. Transition energies and oscillator strengths for electronic excitation to the first 20 singlet excited states of [Zn^{II}ATSM] were calculated using time-dependent density functional theory (TD-DFT) as implemented in ADF.[46]

X-ray Crystallography: Crystals were mounted on a glass fibre and cooled rapidly to 150 K in a stream of cold N_2 using an Oxford Cryosystems CRYOSTREAM unit. Diffraction data was measured using an Enraf–Nonius Kappa CCD diffractometer (graphite-monochromated Mo-K_α radiation, λ = 0.71073 Å). Intensity data was processed using the DENZO-SMN package.[47]

Space groups were identified by examination of the systematic absences in the intensity data. The structures were solved using the direct methods program SIR92,[48] which located all non-hydrogen atoms. Subsequent full-matrix least-squares refinement was carried out using the CRYSTALS program suite.[49] Coordinates and anisotropic thermal parameters of all non-hydrogen atoms were refined. The NH hydrogen atoms were located in the difference Fourier map and their coordinates and isotropic thermal parameters were subsequently refined. Other hydrogen atoms were positioned geometrically after each cycle of refinement. A three-term Chebychev polynomial weighting Scheme was applied. Images were generated using ORTEP-3.[50]

CCDC-671268 [for 4-ethyl-6-methyl-5-methylene-4,5-dihydro-1,2,4-triazine-3(2*H*)-thione] and -671269 [for 2,3-butanedione mono(4-ethylthiosemicarbazone)] contain the supplementary crystallographic data for this paper. These data can be obtained free

of charge from The Cambridge Crystallographic Data Centre via www.ccdc.cam.ac.uk/data_request/cif.

Supporting Information (see also the footnote on the first page of this article): Selected X-ray crystallographic data, DFT-optimised Cartesian coordinates and details of the gradient HPLC method.

Acknowledgments

Thanks are due to all members of the J. R. D. and J. C. G. groups at the University of Oxford. J. P. H. thanks Merton College (Oxford) and the Engineering and Physical Sciences Research Council (EPSRC) for a studentship. S. R. B. thanks Siemens Molecular Imaging Ltd. for a fellowship. H. M. B. and P. J. B. thank GlaxoSmithKline for funding. We thank Prof. Eric J. L. McInnes and Prof. David Collison at the University of Manchester. We thank Mr Mick Woodcock (Gray Cancer Institute) for provision of HeLa cells and Dr Parvinder Aley for assistance with confocal microscopy. We are indebted to Prof. David J. Watkin, Dr. Nick Rees, Mr. Colin Sparrow and Mrs. Maria Marshall for technical support. We also thank the Oxford Supercomputing Centre.

[1] G. Bahr, E. Hess, *Z. Anorg. Allg. Chem.* **1952**, *268*, 351.
[2] G. J. Van Giessen, H. G. Petering, *J. Med. Chem.* **1968**, *11*, 695.
[3] D. H. Petering, *Bioinorg. Chem.* **1972**, *1*, 255.
[4] C. H. Chan-Stier, D. Minkel, D. H. Petering, *Bioinorg. Chem.* **1976**, *6*, 203.
[5] D. T. Minkel, D. H. Petering, *Cancer Res.* **1978**, *38*, 117.
[6] D. T. Minkel, C. Chan-Stier, D. H. Petering, *Mol. Pharmacol.* **1976**, *12*, 1036.
[7] S. V. Smith, *J. Inorg. Biochem.* **2004**, *98*, 1874.
[8] P. J. Blower, J. S. Lewis, J. Zweit, *Nucl. Med. Biol.* **1996**, *23*, 957.
[9] D. X. West, A. E. Liberta, S. B. Padhye, R. C. Chikate, P. B. Sonawane, A. S. Kumbhar, R. G. Yerande, *Coord. Chem. Rev.* **1993**, *123*, 49.
[10] F. Dehdashti, W. Grigsby Perry, A. Mintun Mark, S. Lewis Jason, A. Siegel Barry, J. Welch Michael, *Int. J. Radiat. Oncol. Biol. Phys.* **2003**, *55*, 1233.
[11] F. Dehdashti, M. A. Mintun, J. S. Lewis, J. Bradley, R. Govindan, R. Laforest, M. J. Welch, B. A. Siegel, *Eur. J. Nucl. Med. Mol. Imaging* **2003**, *30*, 844.
[12] J. L. Tatum, G. J. Kelloff, R. J. Gillies, J. M. Arbeit, J. M. Brown, K. S. C. Chao, J. D. Chapman, W. C. Eckelman, A. W. Fyles, A. J. Giaccia, R. P. Hill, C. J. Koch, M. C. Krishna, K. A. Krohn, J. S. Lewis, R. P. Mason, G. Melillo, A. R. Padhani, G. Powis, J. G. Rajendran, R. Reba, S. P. Robinson, G. L. Semenza, H. M. Swartz, P. Vaupel, D. Yang, B. Croft, J. Hoffman, G. Liu, H. Stone, D. Sullivan, *Int. J. Radiat. Biol.* **2006**, *82*, 699.
[13] A. Obata, S. Kasamatsu, J. S. Lewis, T. Furukawa, S. Takamatsu, J. Toyohara, T. Asai, M. J. Welch, S. G. Adams, H. Saji, Y. Yonekura, Y. Fujibayashi, *Nucl. Med. Biol.* **2005**, *32*, 21.
[14] J. P. Holland, F. I. Aigbirhio, H. M. Betts, P. D. Bonnitcha, P. Burke, M. Christlieb, G. C. Churchill, A. R. Cowley, J. R. Dilworth, P. S. Donnelly, J. C. Green, J. M. Peach, S. R. Vasudevan, J. E. Warren, *Inorg. Chem.* **2007**, *46*, 465.
[15] J. P. Holland, J. C. Green, J. R. Dilworth, *Dalton Trans.* **2006**, 783.
[16] J. L. J. Dearling, P. J. Blower, *Chem. Commun.* **1998**, 2531.
[17] J. L. J. Dearling, J. S. Lewis, G. E. D. Mullen, M. J. Welch, P. J. Blower, *J. Biol. Inorg. Chem.* **2002**, *7*, 249.
[18] A. Obata, E. Yoshimi, A. Waki, J. S. Lewis, N. Oyama, M. J. Welch, H. Saji, Y. Yonekura, Y. Fujibayashi, *Ann. Nucl. Med.* **2001**, *15*, 499.
[19] A. R. Cowley, J. R. Dilworth, P. S. Donnelly, E. Labisbal, A. Sousa, *J. Am. Chem. Soc.* **2002**, *124*, 5270.
[20] A. R. Cowley, J. Davis, J. R. Dilworth, P. S. Donnelly, R. Dobson, A. Nightingale, J. M. Peach, B. Shore, D. Kerr, L. Seymour, *Chem. Commun.* **2005**, 845.
[21] J. C. Sheehan, W. A. Bolhofer, *J. Am. Chem. Soc.* **1950**, *72*, 2786.
[22] G. Abbenante, R. H. Prager, *Aust. J. Chem.* **1992**, *45*, 1791.
[23] J. P. Scovill, *Phosphorus, Sulphur, Silicon Relat. Elem.* **1991**, *60*, 15.
[24] M. Christlieb, H. J. Claughton, A. R. Cowley, J. M. Heslop, J. R. Dilworth, *Transition Met. Chem.* **2006**, *31*, 88.
[25] L. Alsop, A. R. Cowley, J. R. Dilworth, P. S. Donnelly, J. M. Peach, J. T. Rider, *Inorg. Chim. Acta* **2005**, *358*, 2770.
[26] L. E. Warren, S. M. Horner, W. E. Hatfield, *J. Am. Chem. Soc.* **1972**, *94*, 6392.
[27] S. Stoll, A. Schweiger, *J. Magn. Reson.* **2006**, *178*, 42.
[28] F. H. Allen, O. Kennard, D. G. Watson, L. Brammer, A. G. Orpen, R. Taylor, *Phys. Org. Chem.* **1987**, S1.
[29] Bruker, *Win-EPR SimFonia*, version 1.26 beta; http://www.bruker-biospin.com/simfonia.html.
[30] D. X. West, J. S. Ives, G. A. Bain, A. E. Liberta, J. Valdes-Martinez, K. H. Ebert, S. Hernandez-Ortega, *Polyhedron* **1997**, *16*, 1895.
[31] Y. Fujibayashi, H. Taniuchi, Y. Yonekura, H. Ohtani, J. Konishi, A. Yokoyama, *J. Nucl. Med.* **1997**, *38*, 1155.
[32] ADF2006.01, SCM, Theoretical Chemistry, Vrije Universiteit, Amsterdam, The Netherlands, **2006**; http://www.scm.com/.
[33] S. I. Gorelsky, *SWizard program*; http://www.sg-chem.net/, Department of Chemistry, York University, Toronto, ON, Canada, **1998**.
[34] O. Couturier, A. Luxen, J.-F. Chatal, J.-P. Vuillez, P. Rigo, R. Hustinx, *Eur. J. Nucl. Med. Mol. Imaging.* **2004**, *31*, 1182.
[35] M. J. Adam, D. S. Wilbur, *Chem. Soc. Rev.* **2005**, *34*, 153.
[36] G. S. Lal, G. P. Pez, R. G. Syvret, *Chem. Rev.* **1996**, *96*, 1737.
[37] S. P. Vincent, M. D. Burkart, C.-Y. Tsai, Z. Zhang, C.-H. Wong, *J. Org. Chem.* **1999**, *64*, 5264.
[38] G. S. Lal, *J. Org. Chem.* **1993**, *58*, 2791.
[39] H. Teare, E. G. Robins, E. Aarstad, S. K. Luthra, V. Gouverneur, *Chem. Commun.* **2007**, 2330.
[40] M. Christlieb, J. R. Dilworth, *Chem. Eur. J.* **2006**, *12*, 6194.
[41] G. Te Velde, F. M. Bickelhaupt, E. J. Baerends, C. Fonseca Guerra, S. J. A. Van Gisbergen, J. G. Snijders, T. Ziegler, *J. Comput. Chem.* **2001**, *22*, 931.
[42] C. Fonseca Guerra, J. G. Snijder, G. Te Velde, E. J. Baerends, *Theor. Chem. Acc.* **1998**, *99*, 391.
[43] S. H. Vosko, L. Wilk, M. Nusair, *Can. J. Phys.* **1980**, *58*, 1200.
[44] A. D. Becke, *Phys. Rev. A* **1988**, *38*, 3098.
[45] J. P. Perdew, *Phys. Rev. B* **1986**, *33*, 8800.
[46] K. Pernal, O. Gritsenko, E. J. Baerends, *Phys. Rev. A* **2007**, *75*, 012506/1.
[47] Z. Otwinowski, W. Minor, *Methods Enzymol.* **1997**, *276*, 307.
[48] A. Altomare, G. Cascarano, G. Giacovazzo, A. Guagliardi, M. C. Burla, G. Polidori, M. Camalli, *J. Appl. Crystallog.* **1994**, *27*, 435.
[49] P. W. Betteridge, J. R. Carruthers, R. I. Cooper, K. Prout, D. J. Watkin, *J. Appl. Crystallog.* **2003**, *36*, 1487.
[50] L. J. Farrugia, *J. Appl. Crystallogr.* **1997**, *30*, 565.

Received: December 18, 2007
Published Online: March 10, 2008

